

# SPITZER IRS spectra of Virgo early type galaxies: detection of stellar silicate emission.

A. Bressan<sup>1,3,4</sup>, P. Panuzzo<sup>1</sup>, L. Buson<sup>1</sup>, M. Clemens<sup>1</sup>, G. L. Granato<sup>1,4</sup>, R. Rampazzo<sup>1</sup>,  
L. Silva<sup>2</sup>, J. R. Valdes<sup>3</sup>, O. Vega<sup>3</sup>, L. Danese<sup>4</sup>

bressan@pd.astro.it; panuzzo@pd.astro.it; buson@pd.astro.it; clemens@pd.astro.it;  
granato@pd.astro.it; silva@ts.astro.it; jrvaldes@inaoep.mx; ovega@inaoep.mx;  
danese@sissa.it

Received / Accepted

## ABSTRACT

We present high signal to noise ratio *Spitzer* Infrared Spectrograph observations of 17 Virgo early-type galaxies. The galaxies were selected from those that define the colour-magnitude relation of the cluster, with the aim of detecting the silicate emission of their dusty, mass-losing evolved stars. To flux calibrate these extended sources we have devised a new procedure that allows us to obtain the intrinsic spectral energy distribution and to disentangle resolved and unresolved emission within the same object. We have found that thirteen objects of the sample (76%) are passively evolving galaxies with a pronounced broad silicate feature which is spatially extended and likely of stellar origin, in agreement with model predictions. The other 4 objects (24%) are characterized by different levels of activity. In NGC 4486 (M 87) the line emission and the broad silicate emission are evidently unresolved and, given also the typical shape of the continuum, they likely originate in the nuclear torus. NGC 4636 shows emission lines superimposed on extended (i.e. stellar) silicate emission, thus pushing the percentage of galaxies with silicate emission to 82%. Finally, NGC 4550 and NGC 4435 are characterized by polycyclic aromatic hydrocarbon (PAH) and line emission, arising from a central unresolved region. A more detailed analysis of our sample, with updated models, will be presented in a forthcoming paper.

*Subject headings:* – Galaxies: formation and evolution – Galaxies: stellar content – Interstellar medium: dust extinction – Infrared: galaxies

## 1. Introduction

Bressan, Granato & Silva (1998) have suggested that the presence of dusty circumstellar envelopes around asymptotic giant branch (AGB) stars should leave a signature, a clear excess at 10  $\mu\text{m}$ , in the mid infrared (MIR) spectral region

<sup>1</sup>INAF Osservatorio Astronomico di Padova, vicolo dell'Osservatorio 5, 35122 Padova, Italy

<sup>2</sup>INAF Osservatorio Astronomico di Trieste, Via Tiepolo 11, I-34131 Trieste, Italy

<sup>3</sup>INAOE, Luis Enrique Erro 1, 72840, Tonantzintla, Puebla, Mexico

<sup>4</sup>SISSA, via Beirut 4, 34014, Trieste, Italy

of passively evolving stellar systems. Early detections of such an excess were suspected in M32 (Impey et al. 1986) from ground based observations, and in a few ellipticals observed with ISO-CAM (Bregman et al. 1998). The first unambiguous confirmation of the existence of this feature, though barely resolved, was found in the ISO CVF spectrum of NGC 1399 (Bressan et al. 2001). Since AGB stars are luminous tracers of intermediate age and old stellar populations, an accurate analysis of this feature has been suggested as a complementary way to disentangle age and metallicity effects among early type galaxies (Bressan et al. 1998; 2001). More specifically, Bressan et al.'s

models show that a degeneracy between metallicity and age persists even in the MIR, since both age and metallicity affect mass-loss and evolutionary lifetimes on the AGB. While in the optical age and metallicity need to be anti-correlated to maintain a feature unchanged (either colour or narrow band index), in the MIR it is the opposite: the larger dust-mass loss of a higher metallicity simple stellar population (SSP) must be balanced by its older age. Thus a detailed comparison of the MIR and optical spectra of passively evolving systems constitutes perhaps one of the cleanest ways to remove the degeneracy. Besides this simple motivation and all other aspects connected with the detection of evolved mass-losing stars in passive systems (e.g. Athey et al. 2002), a deep look into the mid infrared region may reveal even tiny amounts of activity. In this letter we present the detection of extended silicate features in a sample of Virgo cluster early type galaxies, observed with the IRS instrument<sup>1</sup> (Houck et al. 2004) of the *Spitzer Space Telescope*. (Werner et al. 2004).

## 2. Observations and data reduction

Standard Staring mode short SL1 ( $7.5\mu\text{m}$ - $15.3\mu\text{m}$ ), SL2 ( $5\mu\text{m}$ - $7.6\mu\text{m}$ ) and long LL2 ( $14.1\mu\text{m}$ - $21.3\mu\text{m}$ ), low resolution ( $R\sim 64$ - $128$ ) IRS spectral observations of 17 early type galaxies, were obtained during the first *Spitzer* General Observer

<sup>1</sup>The IRS was a collaborative venture between Cornell University and Ball Aerospace Corporation, funded by NASA through the Jet Propulsion Laboratory and the Ames Research Center

Table 1: Virgo galaxies observed with IRS

Name	$V_T$	Date	SL1/2 60s	LL2 120s	S/N $6\mu\text{m}$ .
NGC 4339	11.40	Jun 06 2005	20	14	39
NGC 4365	9.62	Jan 10 2005	3	3	57
NGC 4371	10.79	Jun 01 2005	9	10	40
NGC 4377	11.88	Jun 01 2005	12	8	54
NGC 4382	9.09	Jul 07 2005	3	3	59
NGC 4435	10.66	Jun 01 2005	3	5	35
NGC 4442	10.30	Jan 10 2005	3	3	46
NGC 4473	10.06	Jun 01 2005	3	3	55
NGC 4474	11.50	Jun 01 2005	20	14	38
NGC 4486	8.62	Jun 03 2005	3	3	80
NGC 4550	11.50	Jun 03 2005	20	14	42
NGC 4551	11.86	Jun 03 2005	20	14	47
NGC 4564	11.12	Jun 07 2005	4	6	51
NGC 4570	10.90	Jun 06 2005	3	5	42
NGC 4621	9.81	Jan 12 2005	3	3	63
NGC 4636	9.49	Jul 08 2005	3	5	30
NGC 4660	11.11	Jan 11 2005	3	5	40

Cycle. The galaxies were selected among those that define the colour magnitude relation of Virgo cluster (Bower, Lucy & Ellis 1992). The observing log is given in Table 1. We also report, in columns 4 and 5, the number of cycles of 60 and 120 seconds exposures performed with SL1/2 and LL2, respectively. The spectra were extracted within a fixed aperture ( $3''.6\times 18''$  for SL) and calibrated using custom made software, tested against the SMART software package (Higdon et al. 2004).

The on-target exposures in each SL segment (e.g. SL1) also provide  $\sim 80''$  offset sky spectra in the complementary module (e.g. SL2) that were used to remove the sky background from the source spectrum in the corresponding segment. Since for the LL module we have obtained only LL2 observations, LL2 spectra were sky-subtracted by differencing observations in the two nod positions.

### 2.1. Flux calibration for extended sources

The IRS pipeline version S12 (and older versions) is designed for point source flux extraction. We present here an alternative procedure that exploits the large degree of symmetry that characterizes the light distribution in early type galaxies.

We first obtained the real  $e^-/\text{sec}$  to Jy conversion following the procedure outlined by Kennicutt et al. (2003). We have corrected the conversion table provided for point sources by applying the corrections for aperture losses (ALCF) and slit losses (SLCF). The ALCF is due to the residual flux falling outside the aperture selected in the standard calibration pipeline. To estimate the ALCF we used 4 calibration stars (HR 2194, HR 6606, HR 7341 and HR 7891) observed with *Spitzer* IRS. Using the *Spitzer* Science Center SPICE software package we have evaluated the correction resulting from the average ratio of the fluxes extracted within the standard aperture and within twice the standard aperture. The SLCF correction is applied to retrieve the real flux of an observed point source that hits the slit, accounting for the slit losses due to the point spread function of the optical combination (SLCF). It is defined as the wavelength dependent ratio between the whole flux of a point source on the field of view and the flux selected by the slit to hit the detector. To obtain this correction we have simulated the point spread function of the system (PSF) using the

Spitzer-adapted *Tiny Tim* code and adopting a “hat” beam transmission function of the slit.

After the ALCF and SLCF corrections were applied we obtained the flux *received* by the slit within a given aperture. The estimate of the flux *emitted* by an extended source within the selected angular aperture of the slit involves the deconvolution of the received flux with the PSF of the instrument. This correction is important to obtain the shape of the intrinsic spectral energy distribution (SED) of the galaxy, because from the SLCF we have estimated that for a point source the losses due to the PSF amount to about 20% at  $5\mu\text{m}$  and to about 40% at  $15\mu\text{m}$ . Conversely, a uniform source will not suffer net losses. In order to recover the intrinsic SED we have convolved a surface brightness profile model with the PSF, and we have simulated the corresponding observed linear profile along the slits, taking into account the relative position angles of the slits and the galaxy. The adopted profile is a wavelength dependent two dimensional modified King’s law (Elson et al. 1987):

$$I \equiv I_0 / \left[ 1 + \frac{X^2}{R_C^2} + \frac{Y^2}{(R_C \times b/a)^2} \right]^{-\gamma/2} \quad (1)$$

where  $X$  and  $Y$  are the coordinates along the major and minor axis of the galaxies,  $b/a$  is the axial ratio taken from the literature.  $I_0$ ,  $R_C$  and  $\gamma$  are free parameters that are functions of the wavelength and are obtained by fitting the observations with the simulated profile. In order to get an accurate determination of the parameters of the profiles several wavelength bins have been co-added. This procedure has a twofold advantage because it allows us to (i) reconstruct the intrinsic profile and the corresponding SED and, (ii) to recognise whether a particular feature is resolved or not. The spectrum, extracted in a fixed width around the maximum intensity, is corrected by the ratio between the intrinsic and observed profile. Since for the LL2 segment the above procedure is generally not as stable as for SL segments, we have preferred to fix  $R_C$  to the corresponding value derived in the nearby wavelength region of the SL segment.

An estimate of the signal to noise (S/N) ratio was performed by considering two sources of noise: the instrumental plus background noise and the poissonian noise of the source. The former

was evaluated by measuring the variance of pixel values in background-subtracted coadded images far from the source. The poissonian noise of the sources was estimated as the square root of the ratio between the variance of the number of  $e^-$  extracted per pixel in each exposure, and the number of the exposures. The total noise was obtained by summing the two sources in quadrature and by multiplying by the square root of the extraction width in pixels. The corresponding S/N ratio at  $6\mu\text{m}$  is shown in column 6 of Table 1.

Finally we notice that the overall absolute photometric uncertainty of IRS is 10%, while the slope deviation within a single segment (affecting all spectra in the same way) is less than 3% (see the Spitzer Observer Manual).

### 3. Results

The final flux calibrated spectra of the selected Virgo cluster early type galaxies are shown in Figures 1 and 2.

#### 3.1. Silicate emission from evolved stars

In Figure 1 we have collected the thirteen galaxies (76% of the sample) whose IRS spectra are characterised by the presence of a broad emission feature around  $\lambda \sim 10\mu\text{m}$  that extends toward longer wavelengths. These galaxies show neither PAH features nor emission lines. The observed spectra (solid lines) are superimposed on old SSP from Bressan et al. (1998) normalized at  $\lambda \sim 5.3\mu\text{m}$ . The dotted line is a 10 Gyr,  $Z=0.02$  (solar metallicity) SSP computed without accounting for dusty circumstellar envelopes. Dashed lines from bottom to top refer to 10 Gyr SSPs with increasing metallicity  $Z=0.008$ ,  $Z=0.02$  and  $Z=0.05$ , computed with dusty silicate circumstellar envelopes. The models that account for dusty circumstellar envelopes show an extended feature due to silicate emission, which is very similar to that observed. The feature gets stronger at decreasing age and/or at increasing metallicity due to the corresponding higher dust mass loss rate of the SSP. Since, in addition to the match with the models, the analysis of the intrinsic spatial profile indicates that the whole spectrum is extended, we argue that the observed features are of stellar origin and most likely arise from dusty circumstellar envelopes of mass-losing, evolved stars.

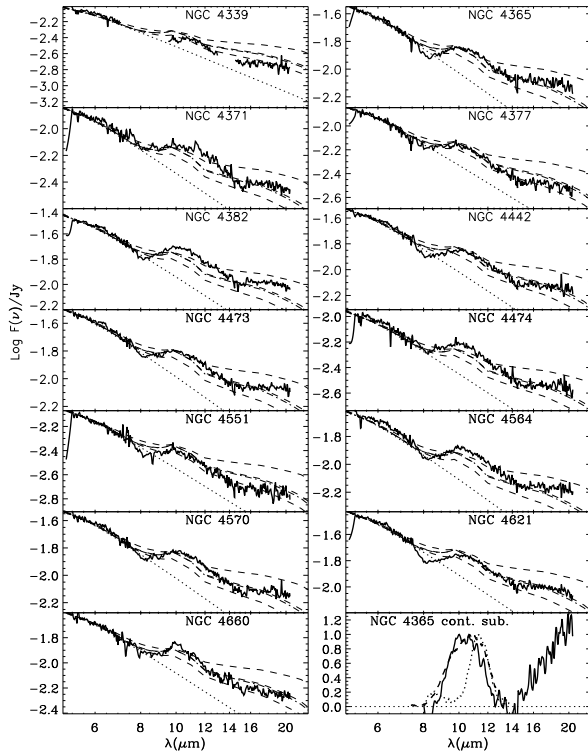


Fig. 1.— IRS spectra (solid lines) of *passively evolving* early-type galaxies in the Virgo cluster. Superimposed are SSP models from Bressan et al. (1998) normalized at  $5.5\mu\text{m}$ . The dotted line is a 10 Gyr,  $Z=0.02$  SSP computed without accounting for dusty circumstellar envelopes. Dashed lines from bottom to top are 10 Gyr SSPs with metallicity  $Z=0.008$ ,  $Z=0.02$  and  $Z=0.05$  respectively, computed with dusty circumstellar envelopes. The dot-dashed line is a young (5 Gyr) metal poor ( $Z=0.008$ ) SSP intended to show that also the MIR spectral region suffers from degeneracy. The bottom right panel compares the normalized continuum subtracted spectrum of NGC 4365 with the normalized continuum subtracted spectrum of the *mean outflow* AGB star (dashed line, Molster et al. 2002) and the carbon rich star U Cam (dotted line, Sloan et al. 1998). For NGC 4365 the pseudo-continuum is a straight line that interpolates the observed spectrum between  $\lambda=8\mu\text{m}$  and  $\lambda=13.5\mu\text{m}$ . The spectrum of NGC 4339 is affected by poorly corrected droops caused by a star falling in the peakup.

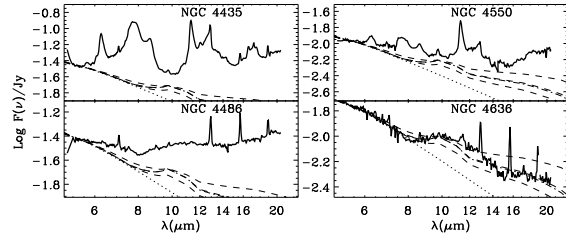


Fig. 2.— IRS spectra (solid lines) of *active* early-type galaxies in Virgo. Models are as in Figure 1.

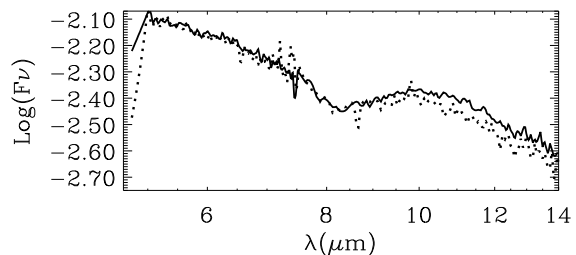


Fig. 3.— IRS spectra of NGC 4551 (dotted line) is compared with that of NGC 4365 (solid line). Spectra are normalized at  $\lambda=5.3\mu\text{m}$ . The silicate features in NGC 4551 are less pronounced than in the case of NGC 4365, indicating a smaller dust mass-loss rate that can be attributed either to an older age or to a lower metallicity.

To corroborate this possibility we compare, in Fig. 1, the normalized continuum-subtracted  $10\mu\text{m}$  silicate emission of the *mean outflow* oxygen-rich AGB star (Molster et al. 2002) and of U Cam (a carbon rich star with SiC emission, Sloan et al. 1998) with that of NGC 4365. Though early type galaxies are expected to harbour carbon stars, given the wide metallicity spread within a galaxy, it seems that the dominant contribution comes from evolved M giants. More detailed models, fully accounting for the expected mixture of evolved stars, will be presented in a forthcoming paper.

The MIR view of early type galaxies proves to be a strong diagnostic for the population content of these galaxies. Recently Temi et al. (2005) noticed that the IRAC flux ratios at  $8\mu\text{m}$  and  $3.6\mu\text{m}$  or MIPS  $24\mu\text{m}$  to IRAC  $3.6\mu\text{m}$  flux ratio remain fairly constant in early type galaxies which otherwise show different  $H\beta$  strength. They conclude that this disagreement supports a small rejuvenation episode. Although this is one of the possibilities invoked by Bressan et al. (1996) to explain early type galaxies with strong Balmer line absorptions, caution must be paid before drawing definite conclusions. Indeed, we show in Figure 1 that a young (5 Gyr) more metal poor ( $Z=0.008$ ) SSP, dot-dashed line, is very similar to an old, more metal rich one. Thus even the mid infrared spectral region is degenerate and in order to break the age-metallicity degeneracy in passively evolved systems a careful combined optical (including possibly NIR) and MIR analysis is required. To further illustrate the strength of this kind of analysis, we show in Figure 3 a comparison of the IRS spectra of NGC 4551 and NGC 4365. A recent optical spectroscopic study (Yamada et al. 2006) indicates that NGC 4551 is significantly younger and more metal rich than NGC 4365. In this case we would expect NGC 4551 to be richer in bright mass-losing AGB stars than NGC 4365, and its silicate features to be more prominent. However, the opposite is observed, suggesting that NGC 4551 is either older or more metal poor (or both) than NGC 4365. Evidently, the effects of degeneracy in the optical can be strong (see e.g. Denicoló et al. 2005, Annibali et al. 2006).

We finally notice that NGC 4473 was observed by ISO (Xilouris et al. 2004) and shows spatially extended emission at  $6.7$  and  $15\mu\text{m}$ . These authors

measured a  $15\mu\text{m}$  excess with respect to SSP models *without* dusty circumstellar envelopes. The excess was interpreted as due to hot diffuse interstellar dust. IRS spectra, such as those presented here, permit the disentangling of the contribution of evolved AGB stars and the presence of interstellar dust.

### 3.2. Active galaxies

The remaining four galaxies (24% of the sample) display different signatures of *activity* in the MIR spectra (Figure 2). These galaxies are classified as active from optical studies (from AGN to transition Liner-HII) at odds with the former group. The spectra of NGC 4636 and NGC 4486 (M 87) show emission lines ([ArII] $7\mu\text{m}$ , [NeII] $12.8\mu\text{m}$ , [NeIII] $15.5\mu\text{m}$  and [SIII] $18.7\mu\text{m}$ ) possibly of non-stellar origin. The broad continuum feature at  $10\mu\text{m}$  in NGC 4486 is not spatially extended and likely due to silicate emission from the dusty torus (Siebenmorgen et al. 2005; Hao et al. 2005). Line emission in NGC 4636 falls on top of the circumstellar emission SED and, as for NGC 4473, its excess at  $15\mu\text{m}$  is of stellar origin and not due to emission by hot diffuse dust as suggested by Ferrari et al. (2002).

The spectrum of NGC 4550 shows PAH emissions features (at  $6.2$ ,  $7.7$ ,  $8.6$ ,  $11.3$  and  $12.7\mu\text{m}$ ) and the  $\text{H}_2$  S(5)  $6.9\mu\text{m}$  and S(3)  $9.66\mu\text{m}$  emission lines. NGC 4435 shows a typical star-forming spectrum. A preliminary interpretation suggests that an unresolved starburst is dominating the MIR emission (Panuzzo et al. in preparation).

## 4. Conclusions

We presented *Spitzer* MIR IRS spectra of early type galaxies selected along the colour-magnitude relation of the Virgo cluster.

We have reconstructed the intrinsic SED of these galaxies from the observed spatial profile sampled by the slits, via a careful analysis of PSF effects. In this way we are also able to differentiate between spatially resolved and unresolved regions within the spectrum. This provides independent support for the interpretation of their nature.

Most of the galaxies (76%) show an excess at  $10\mu\text{m}$  and longward which appears spatially extended and is likely due to silicate emission. This class of spectra do not show any other emission

features. We argue that the  $10\mu\text{m}$  excess arises from mass-losing evolved stars, as predicted by adequate SSP models. A detailed modelling of these features together with the analysis of combined optical, NIR and MIR spectra will be presented in a forthcoming paper.

In the remaining smaller fraction (24%) we detect signatures of *activity* at different levels. We observe line emission superimposed on the stellar silicate features in NGC 4636, unresolved line and silicate emission in M 87 that likely originate in the dusty torus and unresolved PAH emission in NGC 4550 and NGC 4435. The latter galaxy displays the main characteristics of a nuclear starburst (Panuzzo et al. in preparation).

If we exclude M 87, which is a well known AGN, only two out of 16 early-type galaxies observed show PAHs, which corresponds to quite a low fraction ( $\sim 12\%$ ) of the observed sample. It is premature to conclude that such a low fraction of galaxies with PAHs is representative of the cluster early-type galaxy population, especially if we consider that our investigation is limited to the brightest cluster members (the upper two magnitudes of the colour-magnitude relation). A detailed comparison of our results with those obtained for field galaxies will cast light on the role of environment in the galaxy evolution process.

This work is based on observations made with the Spitzer Space Telescope, which is operated by the JPL, Caltech under a contract with NASA. We thank J.D.T. Smith for helpful suggestions on the IRS flux calibration procedure and the anonymous referee for useful suggestions. A. B., G.L. G. and L. S. thank INAOE for warm hospitality.

## REFERENCES

- Annibali, F., Bressan, A., Rampazzo, R. Danese, L., & Zeilinger, W.W. 2006, A&A, submitted
- Athey, A., Bregman, J., Bregman, J., Temi, P., & Sauvage, M. 2002, ApJ, 571, 272
- Bregman, J. N., Athey, A. E., Bregman, J.D., & Temi, P. 1998, AAS, 193, 0903
- Bower, R. G., Lucey, J. R., & Ellis, R. S. 1992, MNRAS, 254, 601
- Bressan, A., Chiosi, C., & Tantalo, R. 1996, A&A, 311, 425
- Bressan, A., Granato, G.L., & Silva, L. 1998, AA, 332, 135
- Bressan, A. et al. 2001, Ap&SS, 277, 251
- Denicoló, G., Terlevich, R., Terlevich, E., Forbes, D. A., & Terlevich, A. 2005, MNRAS, 358, 813
- Elson, R. A. W., Fall, S. M., & Freeman, K. C. 1987, ApJ, 323, 54
- Ferrari, F., Pastoriza, M. G., Macchetto, F. D., Bonatto, C., Panagia, N., & Sparks, W. B. 2002, A&A, 389, 355
- Hao, L. et al. 2005, ApJ, 625, L75
- Higdon, S.J.U. et al. 2004, PASP, 116, 975
- Houck, J.R. 2004, ApJS, 154, 18
- Impey, C.D., Wynn-Williams, C.G., & Becklin, E.E. 1986, ApJ, 309, 572
- Kennicutt, R. C. et al. 2003, PASP, 115, 928
- Molster, F. J., Waters, L. B. F. M., & Tielens, A. G. G. M. 2002, A&A, 382, 222
- Siebenmorgen, R., Haas, M., Krügel, E., & Schulz, B. 2005, A&A, 436, L5
- Sloan, G. C., Little-Marenin, I. R., & Price, S. D. 1998, AJ, 115, 809
- Temi, P., Brighenti, F., & Mathews, W.G. 2005, ApJ, 635, L25
- Werner, M.W. et al. 2004, ApJS, 154, 1
- Xilouris, E. M. et al. 2004, A&A, 416, 41
- Yamada, Y., Arimoto, N., Vazdekis, A., & Peletier, R. F. 2006, ApJ, 637, 200

---

This 2-column preprint was prepared with the AAS L<sup>A</sup>T<sub>E</sub>X macros v5.2.